SUPLEMENTAL MATERIALS

Morphological Stability During Electrodeposition

Raúl A. Enrique,* Stephen DeWitt, and Katsuyo Thornton

Department of Materials Science and Engineering,
University of Michigan

(Dated: May 19, 2017)

MODEL AND NUMERICAL METHODS

In this work, we consider a symmetric half cell with individual grains being electrodeposited on a non-reactive substrate in contact with a binary electrolyte. The electrostatic field is determined by the continuity equation of the current, and the deposition rate is governed by Butler-Volmer kinetics. The equations are solved in two steps: first, the electrostatic field and concentration field are updated for the given interfacial geometry based on the current continuity equation (and the diffusion equation, if considered), and then the interfacial positions are updated based on the reaction rate at the surface of the deposit based on the solution obtained in the first step.

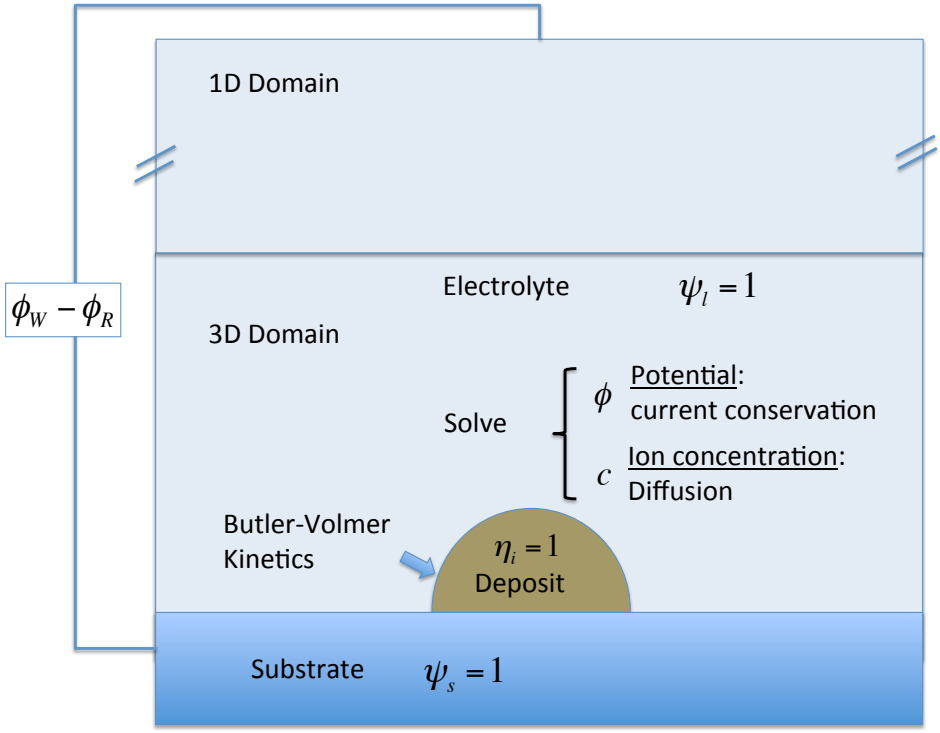

FIG. S1: Schematic illustration of the computational domain employed in the simulations. The electrolyte, deposit, and substrate regions are each identified by a domain parameter. The Cahn-Hilliard and Allen Cahn equations govern the evolution of the domain boundaries. The equations governing the potential and ion concentration fields are solved only in the electrolyte with the deposition/dissolution rate is given by Butler-Volmer kinetics imposed using the smoothed boundary method. The equations governing the electrolyte region is solved fully in three dimensions near the deposit and linked to the one-dimensional solution far away from it.

Figure S1 illustrates the configuration of the computational domain schematically. Each region of the domain is defined by a domain order parameter that takes the value of one inside and zero outside. In this manner, ψ_s represents the substrate, ψ_l the electrolyte, and each grain of the deposit corresponds to a parameter η_i, with *i* ranging from 1 to *p*. Each η_i tracks growth or dissolution of grain *i* during electrodeposition.

Since grains cannot overlap, η_i must not be 1 simultaneously at any point. The free energy functional $\mathcal{F}$ is based on the one proposed for grain growth in polycrystalline solids, which contains a penalty in the form of quadratic functions of η_i in order to impose this condition [1]:

$$\mathcal{F} = \int_V [m f_0(\{\eta_i\}, \psi_l, \psi_s)] + \frac{\kappa}{2}\sum_{i=1}^{p}\left(\nabla \eta_i\right)^2 + \frac{\kappa}{2}\left(\nabla \psi_l\right)^2 \tag{S1}$$

where

$$\begin{aligned} f_0(\{\eta_i\}, \psi_l, \psi_s) &= \sum_{i=1}^{p}\left(\frac{\eta_i^4}{4} - \frac{\eta_i^2}{2}\right) + \left(\frac{\psi_l^4}{4} - \frac{\psi_l^2}{2}\right) + \\ &+ \gamma\sum_{i=1}^{p}\sum_{j>i}^{p}\eta_i^2\eta_j^2 + \gamma\sum_{i=1}^{p}\eta_i^2\psi_l^2 + \gamma\sum_{i=1}^{p}\eta_i^2\psi_s^2 + \gamma\psi_l^2\psi_s^2 + \frac{1}{4}. \end{aligned} \tag{S2}$$

It should be noted that this free energy functional does not represent the thermodynamics of the system, but it is rather employed as a part of the numerical method is to track the evolution of the deposit morphology. Therefore, the parameters that enter into the free energy, as well as the evolution equation based on it, are purely numerical and should not be interpreted physically. For example, the diffuse interface thickness is set to ensure that the interface is numerically resolved for the given resolution, and the mobility is set such that the interfacial evolution is described by the local normal velocity and the order parameter profiles through the diffuse interfaces remain approximately that of the steady state solution. Furthermore, Moelans et al. demonstrated that $\gamma = 1.5$ is a choice that maintains the sum of the order parameters to be approximately one through interfaces and triple junctions [1]. The parameter κ controls the width of the boundaries between different regions. For a planar interface (or grain boundary), the solutions follow a hyperbolic tangent profile:

$$\eta_i(x) = \frac{1}{2}\left[1 - tanh\left(\frac{x}{\delta}\right)\right]. \tag{S3}$$

where the width of the diffuse interface is given by $2\delta = 2\sqrt{\frac{2\kappa}{m}}$. In our simulations, we ensure that 5-6 grid points resolve this distance. The values of the numerical parameters are summarized in Table S1.

Since the substrate is assumed to be stationary, its order parameter, ψ_s, is assumed to be constant. For the domain parameters of the deposits, η_i, we employ the Cahn-Hilliard equation for conserved dynamics to ensure mass conservation of the deposited material. The deposition is treated via a source term:

$$\frac{\partial \eta_i}{\partial t} = \nabla M_{\eta_i} \nabla \frac{\delta \mathcal{F}}{\delta \eta_i} - \vec{v} \cdot \nabla \eta_i, \tag{S4}$$

where v is the local growth velocity of the interface, calculated from the Butler-Volmer equation discussed below.

Since only the electrochemical reaction occurs only on the surface of the deposit exposed to the electrolyte, we write the vector expression for the velocity in terms of the normal (scalar) velocity, v, and the unit normal of the surface calculated as a function of ψ_l,

$$\vec{v} = v\vec{n} = -v \frac{\nabla \psi_l}{|\nabla \psi_l|}. \tag{S5}$$

Thus, the equation governing η_i becomes

$$\frac{\partial \eta_i}{\partial t} = \nabla M_{\eta_i} \nabla \frac{\delta \mathcal{F}}{\delta \eta_i} + v \left(\frac{\nabla \psi_l}{|\nabla \psi_l|} \cdot \nabla \eta_i \right). \tag{S6}$$

The velocity of the interface is related to the reaction current density i_{rxn} through the mass conservation condition. During a time Δt, an element of the deposit surface of area A would sweep a volume of $Av\Delta t$, and mass conservation leads to

$$\frac{i_{\text{rxn}}}{z_+ F} A\Delta t = C_s v A \Delta t, \tag{S7}$$

where C_s is the density of atoms in the metal electrode in the unit of mol per volume, and z_+ is the charge number of the positive ion. By rearranging Eq. S7, we obtain

$$v = \frac{i_{\text{rxn}}}{C_s z_+ F} \tag{S8}$$

Next, we assume that the electrolyte is simply displaced by the growing deposit;

thus, the Allen-Cahn (nonconserved dynamics) equation is used to evolve ψ_l:

$$\frac{\partial \psi_l}{\partial t} = -L_{\psi_l} \nabla \frac{\delta \mathcal{F}}{\delta \psi_l}. \tag{S9}$$

The electrostatic potential, ϕ, in the electrolyte is assumed to be given by the solution to the continuity equation for the current by assuming a dilute binary electrolyte [4]. The current continuity is given by

$$\nabla \cdot \vec{i} = \nabla \cdot \left(z_+ F \vec{J}_+ + z_- F \vec{J}_- \right) = 0. \tag{S10}$$

The flux $\vec{J}_+$ of positive ions is given by

$$\vec{J}_+ = -D_+ \left(\nabla c_+ - \frac{z_+ F}{RT} c_+ \nabla \phi \right) \tag{S11}$$

where c_+ is the concentration of positive ions, D_+ is their diffusivity, and Einstein's relation between diffusivity and mobility is used to eliminate the mobility. An equivalent equation holds for the negative ions. Writing current continuity explicitly and making use of the condition of electroneutrality $z_+ c_+ + z_- c_- = 0$, we have

$$F \nabla \left[(D_+ - D_-) \nabla c_+ + (z_+ D_+ - z_- D_-) \frac{c_+ F}{RT} \nabla \phi \right] = 0, \tag{S12}$$

where c_+ is the concentration, D_- is the diffusivity, and z_- is the charge number of the negative ions. For the scope of the results presented in this paper, which focuses on the development of the instabilities in the absence of concentration depletion (e.g., slow electrodeposition or early stages of rapid electrodeposition), we assume that the concentration of ions is constant, so the first term in the previous equation is ignored. Thus, the conductivity is linearly related to the concentration of positive ions via $\kappa = z_+ c_+ F^2 (z_+ D_+ - z_- D_-) / RT$. In the main text, C_l is used to denote the concentration of positive ions in the electrolyte, i.e., $C_l = c_+$, resulting in Eq. 3 in the main text.

Equation 3 is must be solved with a boundary condition on flux at the reactive surface according to the local reaction rate. As the deposit grows or dissolves, the region occupied by the electrolyte, and thus the reactive surfaces, evolves. As described above, this region is defined by $\psi_l = 1$, and ψ_l is updated via Eq. S9 to follow its evolution. We employ the smoothed boundary method [2], in which the governing equations are

reformulated to satisfy the boundary conditions are automatically. The smoothed boundary method equation for the current is written as

$$\nabla \cdot \left(\psi_l \vec{i} \right) + |\nabla \psi_l| i_{\text{rxn}} = 0, \tag{S13}$$

which then becomes

$$\nabla \psi_l \left[(z_+ D_+ - z_- D_-) \frac{C_l F}{RT} \nabla \phi \right] - |\nabla \psi_l| \frac{i_{\text{rxn}}}{z_+ F} = 0. \tag{S14}$$

The equations are discretized by finite differences. The equations for η_i are solved using a semi-implicit time stepping scheme, in which only the variable for which the rate is calculated for is treated implicitly. The equation for ψ_l is solved explicitly. The electrostatic potential is solved using the method of successive over-relaxation, and the galvanostatic conditions are implemented by iteratively adjusting the potential boundary condition. To reduce the computational cost, the electrolyte domain contains three-dimensional computational domain where the equations are solved fully, which is necessary near the deposit surfaces, and one-dimensional computational domain away from the deposits, where one-dimensional solution accurately describes the solution.

NUMERICAL AND MATERIAL PARAMETERS

Material parameters were chosen to correspond to typical values for Li electrodeposition in battery applications and are summarized in Table I, along with the numerical parameters. In all simulations presented in this paper, the discretization of space is uniform with grid spacing given by $\Delta x = 0.1\ \mu\text{m}$, and the time step is constant and is set to $\Delta t = 0.1\ \text{s}$. The three-dimensional computational domain has a height of 20 μm, which is linked to the one-dimensional computational domain of 900 μm.

TABLE I: Material and Numerical Parameters

Symbol	Description	Value
z	Charge number, $z = z_+ = -z_-$	1
D_+	Diffusivity, positive ions	10^{-6} cm^2 / s [a]
D_-	Diffusivity, negative ions	$D_- = D_+$
i_0	Exchange current density	$1 \sim 10^3$ mA/cm^2
β	Symmetry factor	0.5
C_s	Molar density, electrode	76.93 M
C_l	Ion concentration, electrolyte	0.4 M
Δx		$\Delta x = 0.1\,\mu$m
Δt		0.1 s
M_{η_i}	Cahn-Hillliard η_i mobility	0.1 μm^2 / s
M_{ψ_l}	Allen-Cahn ψ_l coefficient	10^{-2} / s
δ	Diffuse interface width (numerical)	0.28 μm

[a] Set to match conductivity data from Ref. [3]

OVERPOTENTIAL AT THE SURFACE OF THE DEPOSIT

Figure S2 shows the overpotential, defined as $\phi - \phi_w$, at the surface of the deposit for the simulation depicted in Fig. 3 in the main text. The 2D plot shows the values of this overpotential as a function of the height of the deposit. This figure illustrates that variations in overpotential at different points of the surface increase with surface height and that their variation with height is of the order of magnitude of the potential drop over a comparable distance in the electrolyte.

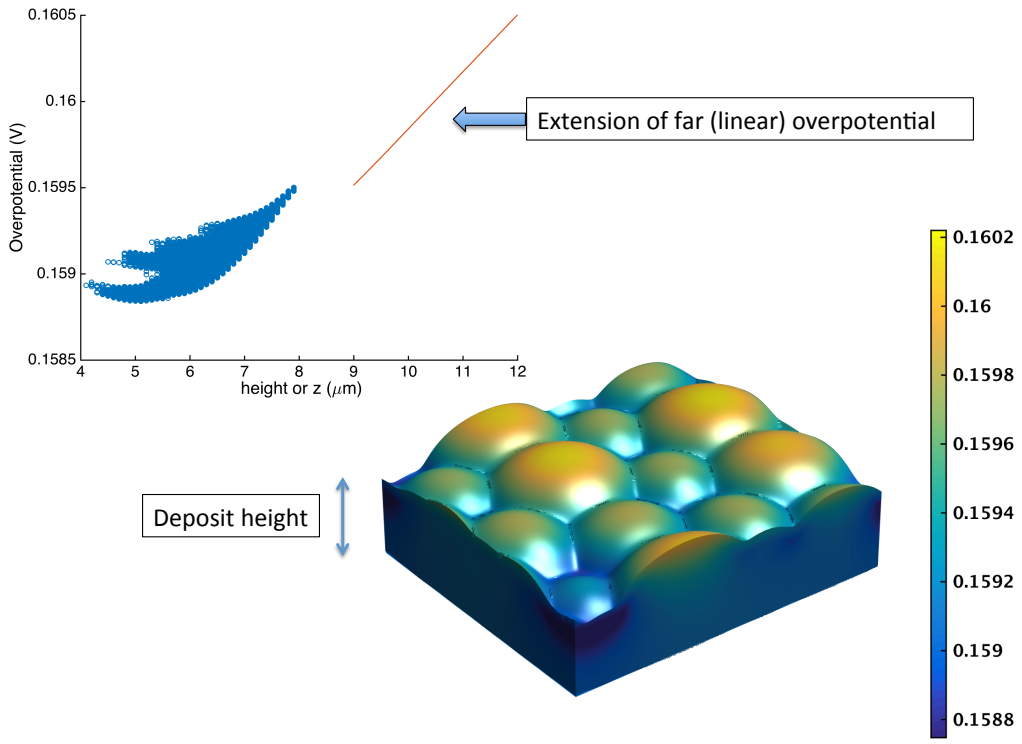

FIG. S2: Overpotential $\phi - \phi_w$ at the deposit surface in eV for the deposit depicted in Fig. 3 in the main text. The upper-left graph is the scatter plot of the value of the overpotential at each grid point at the surface as a function of the height. Far from the deposit, the electrostatic potential varies linearly with the distance to the substrate, and the extension of that linear regime is shown in the plot.

REFERENCES

[1] N. Moelans, B. Blanpain, and P. Wollants, Phys. Rev. B **78**, 024113 (2008).

[2] H.-C. Yu, H.-Y. Chen, and K. Thornton, Model. Simul. Mater. Sci. Eng. **20**, 075008 (2012).

[3] A. M. Christie and C. A. Vincent, J. Phys. Chem. **100**, 4618 (1996).

[4] J. Newman and K. E. Thomas-Alyea, *Electrochemical Systems* (2004).